Journal of Computing and Information Science in Engineering,
Transactions of the ASME, vol. 2, No. 4, December 2002, pp. 312-322.

Hybrid Cellular-functional Modeling of Heterogeneous Objects

Valery Adzhiev
The National Centre for Computer Animation, Bournemouth University, Poole, BH12 5BB UK
vadzhiev@bournemouth.ac.uk

Elena Kartasheva
Institute for Mathematical Modeling, Russian Academy of Science, Moscow, Russia
ekart@imamod.ru

Tosiyasu Kunii
IT Institute, Kanazawa Institute of Technology and Hosei University, Tokyo, Japan
tosi@kunii.com

Alexander Pasko
Hosei University and IT Institute, Kanazawa Institute of Technology
Tokyo, Japan
pasko@k.hosei.ac.jp

Benjamin Schmitt
LaBRI, Bordeaux University I, Talence, France
schmitt@labri.fr

ABSTRACT

An approach to modeling heterogeneous objects as multidimensional point sets with multiple attributes (hypervolumes) is presented. Attributes given at each point represent object properties of arbitrary nature (material, physical, etc.). A proposed theoretical framework is based on a hybrid model of geometry and attributes combining a cellular representation and a functionally based constructive representation of dimensionally non-homogeneous entities. Hypervolume model components such as objects, operations and relations are introduced and outlined. We present examples of modeling a multi-layer geological structure with cavities and wells, time-dependent adaptive mesh generation, and conversion of a 3D implicit complex to the cellular representation.

Keywords

Multidimensional point sets, attributes, heterogeneous models, function representation, cellular representation, volume modeling

1. INTRODUCTION

Modeling heterogeneous objects is becoming an important research topic. Heterogeneous objects are considered in such different areas as modeling of objects with multiple materials and varying material distribution in CAD/CAM and rapid prototyping, representing results of physical simulations, geological and medical modeling, volume modeling and rendering. In this paper, we present an approach to modeling heterogeneous objects as multidimensional point sets with multiple attributes (or *hypervolumes* [1]). We consider real or abstract heterogeneous objects that have internal structure with non-uniform distribution of material and other attributes of an arbitrary nature (photometric, physical, statistical, etc.), and elements of different dimension. It means these objects are heterogeneous from the points of view of structure and dimensionality.

Multidimensional point sets with a fixed dimensionality and with multiple attributes can be quite effectively modeled by the constructive hypervolume model based on real-valued vector-functions as it was recently proposed in [1,2]. The requirement of dimensional heterogeneity naturally brings the idea of adding a kind of cellular representation to the model. Moreover, different applications such as CAD or finite-element analysis require an explicit representation of mixed-dimensional objects along with the functional one. These are the main motivations for introduction of a new hybrid cellular-functional model.

In this paper, we give a concise introduction to the theoretical framework for the hybrid model and provide practical examples illustrating its components. The hybrid model of hypervolumes combines a cellular representation and a constructive representation using real-valued functions. This model allows for independent but unifying representation of geometry and attributes, and makes it possible to represent dimensionally non-homogeneous entities and their cellular decompositions. The hypervolume model components such as objects, operations and relations are introduced and outlined.

To demonstrate a particular application of the proposed framework, we present an example of multi-material modeling – the geological structure with multiple layers, cavities and wells. Another example illustrating the treatment of attributes other than material distributions is concerned with time-dependent adaptive mesh generation where function representation is used to describe object geometry and density of elements in the cellular model of the mesh. The examples have been implemented by using a specialized modeling language and software tools being developed by the authors.

2. OTHER WORKS

We discuss here previous works on modeling objects with varying distribution of material and other attributes, and approaches to modeling dimensionally heterogeneous objects by using cellular representation. Particular attention in solid modeling is paid to modeling objects made of multiple materials with internal material distribution. A non-manifold BRep scheme is used in [3] to subdivide an object into components made of unique materials. Each component is homogeneous inside and has an assigned index of material. Regularized set-theoretic operations are applied to the solid components with the corresponding operations on material indices based on the selection of the resulting material for each pair of materials and for each set-theoretic operation. In the object model proposed in [4], a fiber bundle is used for general description of all characteristics and attributes of an object. Geometry is considered the most fundamental attribute and is represented by an r-set and atlases describing decompositions of the r-set into a finite set of closed 3-cells. The model of attributes is a collection of functions mapping the object geometry to several attributes. The point set together with corresponding attribute models forms a trivial fiber bundle. Constructive operations for

modeling functionally graded materials associated with a BRep geometry model are discussed in [5].

Voxel arrays in volume modeling and graphics can be considered as attribute models with the default geometry represented by a bounding box. Constructive Volume Geometry (CVG) [6] combines geometry and attributes in a systematic manner. The model is presented as algebra of 3D spatial objects utilizing voxel arrays and continuous scalar fields for representing both geometry and photometric attributes (opacity, color, etc.). Issues of modeling volumetric distribution of attributes were addressed in [7-9]. Gradient material distribution represented by scalar functions is combined in [7] with tetrahedral object decomposition and in [9] with a BRep model of the object's 3D geometry. Trivariate NURBS splines are used in [8] to represent both geometry and attributes.

Only 3D static objects and no time dependent or multidimensional objects are considered in the object model, CVG, and other above mentioned methods. Modeling of multidimensional point sets with multiple attributes (hypervolumes) is discussed in [1, 22]. The proposed constructive hypervolume model is based on function representation (FRep) [10] and supports uniform constructive modeling of point set geometry and attributes using real-valued functions of several variables. In this paper, we consider dimensionally heterogeneous objects with multiple attributes. As it was shown in the discussed publications, real-valued functions serve well for modeling both geometry and attributes. However, many applications including CAD and finite-element analysis require explicit representations of geometric elements of different dimension. The main idea of our work is to combine the functionally based and cellular approaches into a single hybrid model.

Cellular models and their construction methods are discussed in a number of publications on shape modeling and solid modeling. Let us mention here just some of them. Multidimensional simplicial complexes are used in [11] for dimension-independent geometric modeling for various applications. A representation of *s*-sets, i.e. finite aggregates of disjoint, open regularized cells, was proposed in [12]. *S*-sets proved to be suitable for modeling assemblies when compared to *r*-sets. Selective Geometric Complex (SGC) [13] is a non-regularized inhomogeneous point set represented through enumeration as the union of mutually disjoint connected open subsets of real algebraic varieties. SGC provides a framework for representing objects of mixed dimensionality possibly having internal structures and incomplete boundaries. The Djinn API for solid modeling [14] is based on cellulary partitioned objects containing mutually disjoint cells which are manifold point-sets of differing dimensionality in 3D. In [15] an extension of B-splines to surfaces of arbitrary topology is proposed. Polyhedral complexes are used to describe the surface topology and to locate control points which are necessary for definition of basis functions of B-splines. In [16] CW-complexes are used to represent the topological structure of implicit surfaces and solids they bound. The CW-complexes form a topological skeleton of the objects describing the configuration of critical points. A procedure for designing cellular models based on CW-complexes (along with object-orientated implementation) with the emphasis on topology validity of resulting shapes is considered in [17, 18].

3. CELLULAR-FUNCTIONAL HYPERVOLUME MODEL

On the basis of the survey presented in [1], we can formulate the requirements for a general model of hypervolumes that are multidimensional point sets with multiple attributes:

- Independent representation of geometry and attributes; in particular, this means that geometry and attributes can be defined in different domains of an entire point set. Accordingly, we treat an attribute not just as a property of a geometric object but rather a property of a space the attribute is associated with, and a geometric object can or cannot possess (that is to say be susceptible to) a certain attribute;
- Coverage of time-dependent and other multidimensional models;
- Constructive modeling of both point set geometry and attributes using primitives, operations, and relations;
- The ability to model geometry and attributes using real-valued functions (scalar fields).

Here we introduce and discuss a general model of hypervolumes satisfying the requirements listed above. We build a *hybrid* (multirepresentational) model based on combining the advantages of FReps [10] and cellular representations. This model also conforms with, and further develops the volume model [19], hybrid volumes [20], the constructive volume geometry model [6], and the object model [4]. We emphasize the following three main specific requirements concerned with the fact that our framework is supposed to be employed in a number of demanding applications far beyond just rendering:

- *Generality*: there should be minimum restrictions concerning nature and features of geometric objects and attributes. In particular, we aim at covering very diverse geometry such as dimensionally heterogeneous objects (composed of curves, surfaces, solids), objects of a discreet nature, manifolds and non-manifolds, etc. The same is true regarding attributes that can be of a quite broad spectrum – from trivial homogeneous material index to a complicated microstructure and arbitrarily distributed temperature;
- *Uniformity*: there is a need for a framework allowing to deal uniformly with diverse geometry and attributes of a different nature (material, photometric, physical, etc.); such an uniformity being traced on a number of levels of consideration (from mathematical basics to software tools) is important for the practicality of the approach;
- *Validity*: the model should provide preserving invariant properties of geometric objects at all the levels of abstraction. A need for a solid mathematical basis stems from the fact that applications (with phases including computational modeling using, for instance, finite elements analysis) can require dealing with rigorously defined objects with valid (in particular, topologically) shapes and features [17].

Let us describe a general hypervolume model as a triple (O, Φ, W), where O is a set of hypervolume objects, Φ is a set of hypervolume operations, and W is a set of relations for the set of objects. Mathematically, the triple can be treated as an algebraic system. Here we can give just an outline of the formal framework to be further elaborated elsewhere.

A *hypervolume object* can be expressed as a tuple,

$o = (G, A_1, ..., A_k)$,

where G is a multidimensional point set and A_i is an attribute. A complete description of the algebraic system can be found in [1].

To build our theoretical models, we rely heavily upon a proper topological framework. The relevant topological notions are introduced in the Appendix.

3.1 Geometry Model

Let us build a geometry model M_G which relies on a geometric object's *Hybrid Representation* (HRep). Such a representation is built on the basis of two other representations, the object's *Function Representation (FRep)* and the object's *Cellular Representation (CRep*).

3.1.1 Function Representation of Geometry

FRep for geometric object $G \subseteq \Omega$, *where* Ω *is modeling space,* can be expressed as

$$M_{G_F} : G_F = \{X \mid X = (x_1, \ldots, x_n) \in \Omega \subseteq E^n, F(X) \geq 0\},$$

where

$F: X \rightarrow \Re$ is a real-valued defining function of point coordinates. Here, F is at least a C^0 continuous function, which is positive inside the point set G, negative outside, and has zero value on its boundary. So, the entire point set is represented by a single real-valued function that allows for combining constructive solid modeling with scalar field techniques based on the theory of R-functions [10, 21-24]. For *k*-dimensional objects in *nD* space with $k<n$, the main idea is that the function F will be zero only at the points of this object and negative everywhere else. For example, if one wants to describe a straight line segment in 2D space, an equation of a straight line can be used: w(x,y)=ax+by+c. The inequality w≥0 defines a halfplane. Then, $-w^2 \geq 0$ defines the line itself, where in fact the function $-w^2$ is never positive and only becomes zero on the line. The line can be trimmed using some 2D solid to produce one or several segments. The simplest way to define a segment is $-w^2 \wedge_0 g \geq 0$, where $g(x,y) \geq 0$ is a definition of a 2D disk, and '$\wedge_0$' stands for set-theoretic intersection defined by an R-function (see [10, 21, 23]).

Fig.1 shows a dimensionally heterogeneous geometric object, which consists of a disk with three round holes and three dangling line segments attached. FRep of this object is described by a single function F(x,y) ≥0,

$$F=F_{disk} \setminus_0 F_{hole1} \setminus_0 F_{hole2} \setminus_0 F_{hole3} \vee_0 F_{AB} \vee_0 F_{LM} \vee_0 F_{QS},$$

where F_{disk} defines the disc, F_{holei} represents the i^{th} hole, F_{AB}, F_{LM}, F_{QS} describe the line segments, and the symbols $\setminus_0$,$\vee_0$ denote R-functions defining set-theoretic subtraction and union ([10, 21]). The defining functions are as follows:

$F_{disk} = r_0^2-(x-x_0)^2-(y-y_0)^2$

$F_{holei} = r_i^2-(x-x_i)^2-(y-y_i)^2$, i=1,2,3,

where (x_0,y_0) is a center of the disk, r_0 is its radius, (x_i,y_i) , r_i are centers and radii of the holes correspondingly.

According to the approach described above the FRep for segment AB can be written as

$F_{AB}= -(F_{hpAB})^2 \wedge_0 F_{diskAB}$,

where F_{hpAB} defines a halfplane and F_{diskAB} represents a trimming disk:

$F_{hpAB} = (y_A-y_B)x + (x_B-x_A)y + x_Ay_B - x_By_A$,

$F_{diskAB} = (x_B-x_A)^2+ (y_B-y_A)^2 - (x- (x_B+x_A)/2)^2 - (y- (y_B+y_A)/2)^2$.

The other segments are defined in a similar manner.

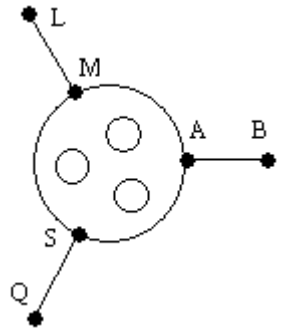

Figure 1: Example of a heterogeneous object in E^2.

The geometric domain of FRep in 3D space includes solids with non-manifold boundaries and lower dimensional entities (surfaces, curves, points) defined by zero value of the function. The lower dimensional elements in 3D space can be defined as follows:

- "implicit" definition of a surface patch requires an "implicit" surface and a trimming 3D solid;
- a curve can be defined as the intersection of two surfaces, each defined as $-f^2 \geq 0$;
- a point can be defined as the intersection of three surfaces, a curve and a surface, or directly as d(x,y,z), where d is a negative distance to the given point.

Rvachev et al. [22] show that such a function representation of dimensionally heterogeneous objects is very useful in solving interpolation and boundary value problems. See also applications in [24].

The main distinctive characteristic of FRep is that the real-valued function defining the point set is evaluated at the given point by a procedure traversing a tree structure with primitives in the leaves and operations in the nodes of the constructive tree. Many operations (set-theoretic, blending, non-linear deformations, metamorphosis, sweeping, hypertexturing, etc.) have been formulated for FRep in such a manner that they yield continuous real-valued functions as output, thus guaranteeing the closure property of the representation. The main relations over functionally defined geometric objects are point membership, inclusion and intersection.

3.1.2 Cellular Representation of Geometry

CRep for geometric object $G \subseteq \Omega$ can be defined as

$$M_{G_C} : G_C = \{ X \mid X \in \Omega \subseteq E^n, X \in |K^q| \},$$

where $K^q = \{C_i^r; r = 0,1,...,q; i = 1,...,I_r\}$ is a q-dimensional CW-complex embedded in a modeling space Ω ($q \leq n$). Such a definition allows for representation of dimensionally heterogeneous objects in the form of union of all point sets associated with all cells of K endowed with subspaces topology of n-dimensional space. All the cells composing K are supposed to be defined by characteristic maps of various types. In principle, a number of cellular decompositions are possible, and there can be applications where it is useful to have more than one

representation for the same geometry. Two examples of various cellular representations of the heterogeneous object introduced in 3.1.1 are shown in Fig.2. Simplicial decomposition (CRep described by a simplicial complex) is illustrated by Fig.2a. and CRep based on a CW-complex is shown in Fig. 2b.

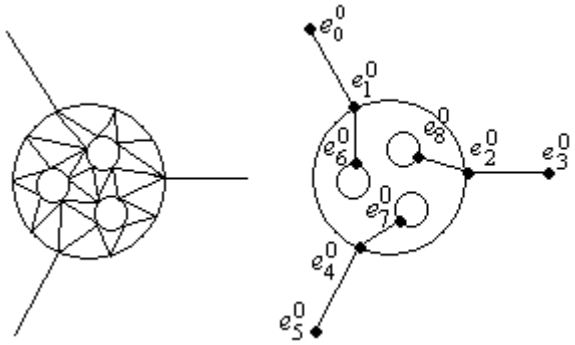

a b

Figure 2: Various cellular representations of the heterogeneous object shown in Fig.1: (a) CRep described by a simplicial complex, (b) CRep described by a CW-complex

Let us describe in more detail the object represented by CW-complex in Fig.2b. It consists of nine null-dimensional cells, twelve one-dimensional cells and one two-dimenisional cell. Points $e^0_0,\ldots,e^0_8$ represent null-dimensional cells of the complex. One-dimensional cells include six open segments (e^0_0 , e^0_1), (e^0_2 , e^0_3), (e^0_4 , e^0_5), (e^0_1 , e^0_6), (e^0_2 , e^0_8), (e^0_4 , e^0_7) and six open arcs (e^0_1 , e^0_2), (e^0_2 , e^0_4), (e^0_4 , e^0_1), (e^0_6 , e^0_6), (e^0_7 , e^0_7), (e^0_8, e^0_8), where (e^0_i , e^0_i) denotes a circle with deleted point e^0_i , i = 6,7,8. Finally, the two-dimensional cell is a disk with holes cut along the segments (e^0_1 , e^0_6), (e^0_2 , e^0_8), (e^0_4 , e^0_7). The operation of composing a cellular complex representing a geometric object irrespective of its nature and features (it can be manifold, non-manifold, etc.) is based on the procedure of attaching cells described in the Appendix.

The main relations defined between elements of a cellular complex are incidence and adjacency. We can consider the relation "to be properly joined" between two cellular complexes (see its definition in the Appendix). Point membership, inclusion and intersection relations are valid for CRep too. All operations defined for CRep can be subdivided into three groups: analysis, synthesis and conversion. The first group includes operations for topological analysis such as determination of connectivity and orientability, evaluation of the homology and homotopy groups, and others [25, 26]. The synthesis operations include cell complexes' generation procedures (described in the Appendix), geometric transformations, set-theoretic operations for properly joined complexes, various reconstructions of complexes (e.g., cell subdivision or collapse, replacement of a subcomplex by another one with the same boundary, optimization of complexes, transformation of a simplicial complex into a cellular one with the same carrier [26], etc.), selection of subcomplexes according to various restrictions (for example, boundary or co-boundary of a cell, boundary of a complex, a common subcomplex for two properly joined complexes, etc.). and topology transformation (e.g., slicing of h-genus surfaces or solids [26]). The third group involves procedures of conversions between FReps and CRep such as evaluation of functional representation for cellular complexes (see the discussion in 3.1.1), polygonization of FReps [27], and tetrahedrization of 3D solids [28].

3.1.3 Hybrid Representation of Geometry

The first step towards more universal representation is to have both FRep and CRep for the same geometric object. Such a dual representation should be supported by conversions of FRep and CRep into each other. The entire cell complex in nD space can be defined as $F(X) \geq 0$, taking into account that lower dimensional cells with dimension k<n have only zero values of the function F at all their points. For each cell, first a set-theoretic representation is constructed, then operations are replaced by R-functions and nodes by the defining functions of primitives, including those with the description $-f^2 \geq 0$ (see the details in the discussion of FRep above). As examples of FRep to CRep conversion, one can mention tetrahedrization of 3D solids and polygonization of 3D solid boundary.

Cellular representation is especially useful when there is a need for information about the object's internal structure or about the object's boundary decomposition. However, such information presented by using explicit schemes can be quite bulky. For instance, when one wants to use complexes to represent an object with dimensionally heterogeneous components, detailed information about their internal subdivision can be redundant.

So, a challenging idea is to integrate both representations into a single genuine hybrid representation (HRep) to get benefits from different representations, which can be merged to complement each other. To make this idea feasible, let us introduce a notion of an *implicit complex*. Such a complex has the following features:

- it is defined as a union of *properly joined* (see Appendix) cellular spaces (which we call *domains* to distinguish them from general cellular spaces);
- subspaces that are shared by two or more domains are represented by explicitly defined cellular subcomplexes; accordingly, some domains can be represented by explicit cellular complexes; for other domains, it is enough to have only a few explicit cells to form a base for the intersection; as to their complete representation, it is defined functionally;
- as all these cellular spaces are properly joined, they ultimately form a complex, which we call an implicit one.

Formally HRep for geometric object $G \subseteq \Omega$ can be defined as

$$M_{G_H} : G_H = \{ X \mid X \in \Omega \subseteq E^n, X \in |K^q|\},$$

where K^q is an implicit q-dimensional complex (representing an object in E^n with maximal dimension $q \leq n$); it can be expressed as:

$$K^q = < C^s, \{(T_i^{k_i}(h_i^{k_i}, F_i^{k_i}), P_i^{m_i})\} > ,$$

where $q=\max(s,k_i)$, i=1,2,..,I, I is the number of implicit subcomplexes, C^s is a s-dimensional explicit subcomplex;
then, for each implicit subcomplex with index i:
T^k is a point set of a k-dimensional domain,
F^k is a function of k arguments defining FRep for the preimage $(T^k)'$ of the point set T^k in E^k,
h^k is an embedding map of E^k to E^n as a homeomorphism taking the preimage $(T^k)'$ to T^k,

P^m denotes the subcomplex with cells belonging to T^k – a domain with dimensionality $m \le \min(k,s)$.

We can record the following properties of K^q:

i. $\forall i : P_i^{m_i} \subset C^s$

ii. $\forall i : (T_i^{k_i} \cap | C^s |) = | P_i^{m_i} |$

iii. $\forall (i, j)$: either $T_i^{k_i} \cap T_j^{k_j} = \varnothing$ or $(T_i^{k_i} \cap T_j^{k_j} = | P_i^{m_i} \cap P_j^{m_j} |)$ (all domains are properly joined)

iv. $\forall i, \forall e_j^p \in C^s$: either $T_i^{k_i} \cap | e_j^p | = \varnothing$ or $(T_i^{k_i} \cap | e_j^p | = | e_j^p \cap P_i^{m_i} |)$ (all domains are properly joined with respect to cells e_j^p of C^s.)

Note, that such a cellular-functional model can be converted to a purely cellular one since each implicit domain being a cellular space by definition, can have a cellular partition, and such a partition can be made independently for each domain.

Let us enumerate some of operations on HRep objects:

- Building objects through composing implicit complexes;
- Converting FRep->CRep (in particular, to CW-complex) and FRep->HRep;
- Converting HRep->CRep (in particular, CW-complex) and HRep->FRep;
- Set-theoretic operations over HRep objects;
- Operations on rebuilding HRep objects (e.g., transformation of the complexes' structure through their subdivision, simplification, etc).

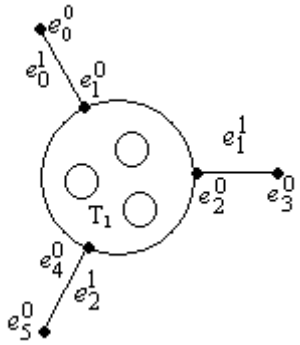

Figure 3: Hybrid representation of the heterogeneous object shown in Fig.1

Let us illustrate the proposed hybrid representation by implicit complexes in 2D and 3D spaces. As Fig. 3 shows, the object introduced in 3.1.1 can be described as the union of two domains: D_1 (represents a 2D disk with holes) and D_2 (represents 1D segments). Obviously, D_2 can be represented explicitly; as to D_1, it is reasonable to use implicit representation with a functionally defined disk with holes plus a complex of three attaching points:

$K^2=<C^1, (T^2_1(F^2_1), P^1_1)>$,
$C^1=\{ e^0_0, e^0_1, e^0_2, e^0_3, e^0_4, e^0_5, e^1_0, e^1_1, e^1_2\}$,
$P^1_1=\{ e^0_1, e^0_2, e^0_4\}$,
$F^2_1=F_1(x,y)=[r_0^2-(x-x_0)^2-(y-y_0)^2] \setminus_0 [(r_1^2-(x-x_1)^2-(y-y_1)^2)]$
$\setminus_0 (r_2^2-(x-x_2)^2-(y-y_2)^2) \setminus_0 [(r_3^2-(x-x_3)^2-(y-y_3)^2)]$,

where

C^1 is the one-dimensional explicit subcomplex defining the explicit domain D_2 (it consists of three one-dimensional cells representing the line segments and six null-dimensional cells representing the end points of the line segments);

P^1_1 is the subcomplex including the cells belonging to the implicit domain D_1;

$F_1(x,y)$ describes the functional model of the implicit domain D_1. Map *h* is omitted as in this case *h* is an identity map.

Fig. 4 shows an example in 3D space where using domains with different dimensionalities are necessary. The object consists of a cylinder with a longitudinal hole and a bent surface patch with a hole, which is attached to the cylinder's surface. Here, we use two implicit domains. The first one, D_1 is represented as a 3D cylinder defined functionally as $F_1(x,y,z)\ge 0$. The explicit part of this domain consists of cells corresponding to two "attaching points" and one "attaching" line segment. The second implicit domain D_2 presents a more interesting case. The point set T_2^2 has its preimage $(T_2^2)'$, which is defined on the plane (u,v) by a function $F_2(u,v)\ge 0$. Then, we must define embedding map h: E^2 -> E^3, which gives us homeomorphism taking $(T_2^2)'$ to T_2^2. The second domain has the same explicit part as the first one. So, the HRep is as follows:

$K^3 = <C^1, \{(T_1^3(F_1), P_1^1), (T_2^2(h, F_2), P_2^1)\}>$,
$P_1^1 = P_2^1 = C^1$,
$C^1 = \{ e^0_1, e^0_2, e^1_1\}$,
h : {x = au+e; y = bsin(cu)+d; z = gv+k;}, a,e,b,c,d,q,k are real value constants.

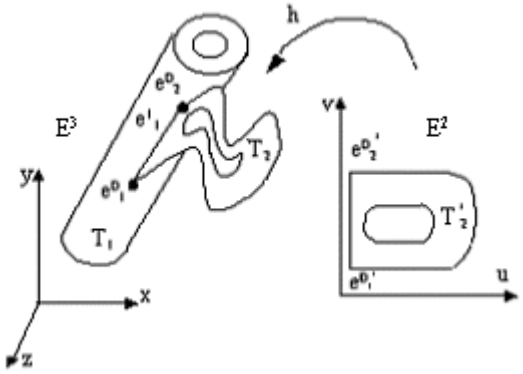

Figure 4: Example of a hybrid representation in E3.

3.2 Attribute Model

Let us build an attribute model M_A. The main principle is to define an attribute at any point of the modeling space. We are not going to impose any other restrictions; as to a meaningful interpretation of a certain attribute, it depends on its nature and specifics. We will introduce three different representations for the attribute model, namely one functional and two cellular-based ones.

3.2.1 Function Representation of Attributes

The generic model for the attribute A_j is a set of values $\mathbb{N}_j$ (which can be a vector or tensor space) embedded into a space $\Re^{m_j}$ of a proper dimension m_j. Each point of the modeling space $\Omega \subset E^n$ is mapped to the attribute value set $\mathbb{N}_j$. Depending on the application, there can be attributes with different domains: some of them are defined at each point of the modeling space (e.g., temperature), whereas others are defined in the subset of modeling

space, in particular, only at points belonging to a geometric object (e.g., material attributes). For the sake of uniformity, we introduce an *extended real space* $\Re_\theta = \Re \cup \{\theta\}$, where θ is "undefined value". By assumption, for any $\rho \in \Re_\theta$, and for any operation o defined in $\Re_\theta$, $\rho o \theta = \theta o \rho = \rho$.

Then, FRep for an attribute A_j can be expressed as

$M_{A_{Fj}} = \{(N_j, S_j)\} : \{A_j = \{ n_j \in \mathcal{N}_j \mid \eta_j = S_j(X),\ X = (x_i, ..., x_n) \in \Omega \} \}$

where $S_j : \Omega \rightarrow \mathcal{N}_j \subseteq \Re_\theta^{m_j}$ is an attribute real-valued defining function of point coordinates (see Fig.5). Depending on a particular attribute, $S_j\ (X)$ can be either C^k, k ≥ 0 or even not necessarily continuous at all.

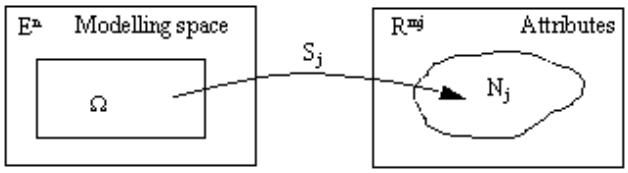

Figure 5: Functional representation of attributes

In the particular case, when one needs to define an attribute as a property of the geometric object G, one can use the map already introduced, which is defined in the entire modeling space with values θ for points not belonging to G.

Note, that different attributes can have both the same and different domains and value spaces. There are no restrictions on operations over attributes in the sense that all operations valid in the corresponding $\Re_\theta^{m_j}$ can be defined. This means it is possible, for instance, to add or subtract values for attributes having "the same type" (that is attributes values are defined in the spaces $\Re^{m_j}$ of the same dimension m_j). So, one can easily deal with multi-component attributes, such as color composed of RGB components. Operations over attribute functions representing materials, in particular material composition operations (similar to ones described in [5]), can easily be introduced too. Note that operations over attributes can be based either on universal functions defined initially for geometry or on specialized library functions (more details can be found in [1,2]). Also, one can define operations over maps themselves thus getting new maps on the base of already available ones.

3.2.2 Cellular-functional Representation of Attributes

If the space is partitioned and defined as an explicit or implicit complex K (or the geometric object is represented by CRep or HRep), then representation for an attribute can also be defined through a map but having a more complicated structure. Namely, such a map can be represented as a collection of maps associated with subcomplexes of the entire complex K in the form of a set of the map's restrictions on K's elements.

Let A_j be an attribute and K_j^q be a corresponding q-dimensional complex (in principle, there can be different partitions for each attribute, although the situation with a single partition for all attributes is possible too). Then a cellular-functional representation for an attribute A_j is as follows:

$M_{A_{CFj}} = \{(N_j,\ K_j^q\ , S_j)\}$:

$\{A_j = \{ nj \in \mathcal{N}_j \mid \eta_j = S_j(X),\ X = (x_i, ..., x_n) \in \mid K_j^q \mid \} \}$,

where $S_j = \{S_{j_i}^r \mid S_{j_i}^r : C_i^r \rightarrow V_i^r \subseteq N_j ; r = 0,1,...,I_r\}$,

and C_i^r is a K's element or an implicit domain with dimensionality r, I_r is a number of such elements, V_i^r is a restriction of a set of the attribute's values corresponding to C_i^r (see Fig.6).

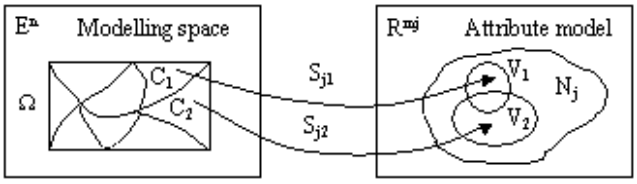

Figure 6: Cellular-functional representation of attributes

Let us consider a simple example concerned with the definition of a material attribute A_m for the geometrical object shown in Fig.4. Let the cylinder part and the bent surface be made of different materials with indexes μ_1, μ_2, correspondingly (μ_1, $\mu_2 \in \mathcal{R}$). Then, material attribute A_m can be associated with the value set N_m=$\{\mu_1$, $\mu_2\}$. Two different descriptions of the material attribute can be constructed: the first one is based on the functional approach and the second one exploits the cellular-functional model.

Namely, the function representation of A_m uses the following attribute function S_f:

$$S_f(x,y,z) = \begin{cases} \mu_1 & if \quad F_1(x,y,z) \geq 0 \\ \mu_2 & if \quad F_1(x,y,z) < 0 \end{cases},$$

where $F_1(x,y,z)$ describes the cylinder part.

The cellular-functional approach results in the attribute map S_H defined as the collection

S_H= $\{S_1, S_2, S_3, S_4, S_5\}$, where

S1: D1->$\{\mu_1\}$*, D1* is the cylinder domain;
S2: D2->$\{\mu_2\}$*, D2* is the bent surface domain;
S3: $e^1{}_1$ -> $\{\mu_1\}$,
S4: $e^0{}_1$ -> $\{\mu_1\}$,
S5: $e^0{}_2$ -> $\{\mu_1\}$.

3.2.3 Cellular Representation of Attributes

The next logical step is to define attributes directly on a complex of one of the introduced types. Here, we can provide just a brief and rather informal outline for such a model. Let K^q be a q-dimensional complex embedded in modeling space $\Omega \subseteq E^n$. If $N_j \subseteq \Re_\theta^{m_j}$ represents a set of values for attribute A_j, then one can build a complex W^q embedded in E^{n+m_j}. This complex can be treated as a model, which represents the modeling space integrating with the attribute. To create such a complex, one can define a homeomorphic map $H_j : K^q \rightarrow W^q$. To get the attribute value from W^q at the given point of the modeling space, we need

to introduce a special *projection* operation $\prod_j : | W^q | \rightarrow N_j$. So, the cellular attribute model can be expressed as:

$$M_{A_C} = \{(N_j, K_j^q, W_j^q, H_j, \Pi_j)\} :$$

$$\{A_j = \{ \quad n_j \in N_j \mid n_j = \Pi_j(H_j(X)),\ X \in | K_j^q | \} \}.$$

If the point $X \notin | K_j^q |$, then the attribute value is assigned to θ.

Fig.7 illustrates this attribute model.

Note that such a cellular representation of attributes can cover as a particular case the cell tuple approach to modeling graded compositions described in [7].

The scheme can be illustrated by the following simple example. If we have a temperature value $\{t_i\}$ in a number of points $\{b_i\}$ in the modeling space $\Omega \subseteq E^2$, then one can triangulate the space Ω using those points as vertices. So, we get a simplicial complex K in E^2. Then, we can build a complex W embedded in E^3 but with the same dimensionality and structure as K – only points change their location in the space. There is one-to-one conformity between vertices $b_i = (bx_i, by_i) \in K$ and $v_i = (vx_i, vy_i, vz_i) \in W$ such that

$v_i = H(b_i)$ and $vx_i = bx_i$, $vy_i = by_i$, $vz_i = t_i$. Then for each point $(x,y) \in \Omega \subseteq E^2$ its image $H(x,y) = (x,y,z) \in E^3$ is defined as follows:

$H(x,y) = \lambda_0 H(b_{i0}) + \lambda_1 H(b_{i1}) + \lambda_2 H(b_{i2})$, where

λ_0, λ_1, λ_2 are the barycentric coordinates of the point (x,y) in the corresponding triangle $(b_{io}, b_{i1}, b_{i2}) \in K$ which it belongs to.

One can get the interpolated temperature value at the point (x,y) as follows:

$t = \prod(x,y,z) = z = \lambda_0 t_{i0} + \lambda_1 t_{i1} + \lambda_2 t_{i2}$.

This temperature attribute is fully independent and can be combined with various geometric objects defined in $\Omega \subseteq E^2$.

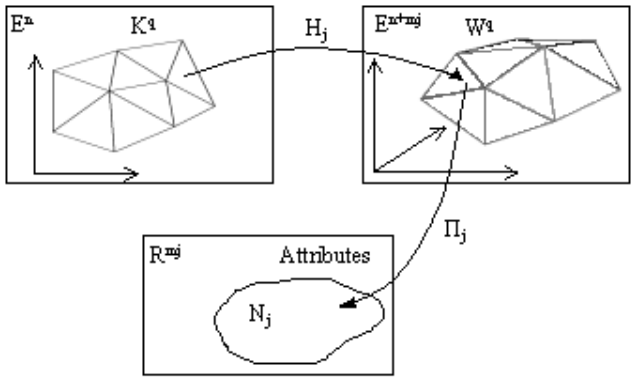

Figure 7: Cellular representation of attributes

In [7] attribute values are rigidly tied with cells defining the object geometry, and the same base functions are applied to approximations of both the object geometry and the object attributes. In our framework, the cellular model of attributes is defined on the base of a cellular complex that is fully independent from the geometry model. So, we can use different cell complexes for descriptions of the geometry and attributes. Moreover, we can combine the cellular model of attributes with the functional or the cellular-functional model of the geometry. For example, we can apply the above introduced cellular model of the temperature field to the geometry model shown in Fig.1. The extended B-spline described in [15] can be considered as another more complicated example of the embedding map H.

3.3 Hybrid Hypervolume Model

Now we can define a unifying *hypervolume model* as a composite (collection) of its geometry and attribute models:

$$M_{HV} = M_G \otimes M_{A_1} \otimes ... \otimes M_{A_j} \otimes ... \otimes M_{A_k},$$

where operator $\otimes$ is a topological product. The component models are heterogeneous:

$$M_G = M_{G_F} \oplus M_{G_C} \oplus M_{G_H},$$

$$M_{A_j} = M_{A_{F_j}} \oplus M_{A_{CF_j}} \oplus M_{A_{C_j}}.$$

Then, a hypervolume object can be modeled as a product set $O_{HV} = G \times (\prod_{j=1}^{k} N_j)$. The mathematical space in which the hypervolume object model O_{HV} is represented can be given as

$$T_{HV} = E^n \times (\prod_{j=1}^{k} E_j^{n+m_j}) \times \prod_{j}^{k} \Re_\theta^{m_j} :$$

Let us summarize the main features of the hypervolume model which make it distinct from the related ones, in particular described in [4, 5, 7]:

- The hybrid hypervolume model is quite versatile. It integrates functional and cellular definitions both for the geometry and attributes that allow us to get benefits from different representations and to create mathematically valid models of a quite broad set of real objects and phenomena.
- The hybrid hypervolume model is inherently multidimensional and also covers dimensionally heterogeneous models.
- In the hybrid hypervolume model, geometry and attributes are completely independent, although they can share the same space. Actually, geometry and attributes each occupy their own part of multidimensional modeling space; these parts can overlap or coincide.

4. CASE STUDIES

In section 3, we have provided examples illustrating the hybrid representation in the form of the implicit complexes (see Figs.1 and 2 in Section 3.1.3). In this section, we describe case studies concerned with practical applications. They allow us to show how such model components as functional models of geometry and attributes (Section 4.1), and conversion between functionally defined and cellular objects (Section 4.2) or between hybrid and cellular objects (section 4.3) can be implemented by using special software tools being developed by the authors.

4.1 Modeling of Geological Structure

Heterogeneous objects in geosciences usually consist of multiple layers of different materials with cavities, wells, and other irregularities. We present here a simplified example of a functional model of such a geological object. There are two steps in making this model: description of the point set geometry and description of material attributes. The basic geometric model

shown in Fig. 8 is described by a single function $F_{geom}(X) \geq 0$, where X is a vector of 3D point coordinates,

$$F_{geom} = F_{relief} \wedge_0 F_{bbox} \wedge_0 (-F_{cavity}) \wedge_0 (-F_{well}) \wedge_0 F_{cut},$$

F_{relief} defines a solid bounded by the top curvilinear surface and the bottom plane, F_{bbox} is a function defining a bounding box for the model, F_{cavity} is a model of cavities made using an algebraic sum between the functions of an ellipsoid and solid noise, F_{well} represents a gas well modeled as union of two cylinders and a toroidal segment, and F_{cut} serves for producing a zigzag cut of the full object. The symbol $\wedge_0$ stands for the R-function defining set-theoretic intersection between two functionally defined solids (see [10, 21]):

$$f_A \wedge_0 f_B = f_A + f_B - \sqrt{f_A^2 + f_B^2}$$

For the model of the "relief" solid, we used the following expression: $F_{relief} = (f_{relief}(x,y) - z) \wedge_0 z$, where $z=f_{relief}(x,y)$ defines the top curvilinear surface of the object, and z value of the bottom plane is zero.

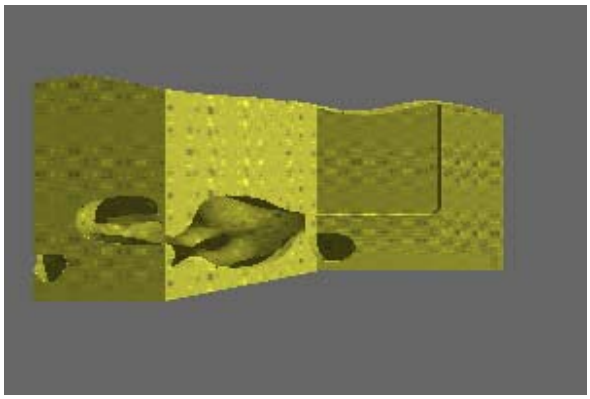

Figure 8: Geological structure: a geometric model without attributes.

The five material layers shown in Fig. 4 using different textures are presented in the attribute model by the space partition different from the basic geometric model. For the i-th layer, the defining function is

$$F_i = (f_{i+1}(x,y) - z) \wedge_0 (-f_i(x,y) + z),$$

where $i=1,4$, $f_5=f_{relief}$, and $z=f_i(x,y)$ defines the top surface of the layer. In the simplest case of the homogeneous material distribution inside the layer, the single material attribute can be defined as

$$A = \begin{cases} M_i, F_{geom} \geq 0, F_i \geq 0 \\ \theta, F_{geom} < 0 \end{cases}$$

where M_i is a material index, and θ stands for the undefined value (see the discussion of the attribute model above). The priority to the material index on the surfaces separating the layers is given by the procedure of scanning the indices for checking the condition $F_i \geq 0$. The complete functional hypervolume model is defined as $o = (F_{geom}, A)$. In fact, the visual appearance of the layers in Fig. 4 is achieved not by attaching surface textures, but is automatically obtained by volume rendering of the hypervolume with the set of attributes assigned to each point instead of the material index.

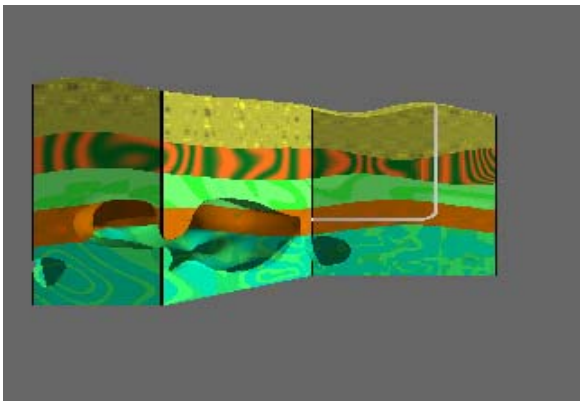

Figure 9: Geological structure: a model with attributes.

The full functional hypervolume model in this case looks like:

$$o = (F_{geom}, A_1, A_2, ..., A_{13}),$$

where A_i are photometric attributes (color components, opacity, etc.). In Fig. 9 trigonometric and quasi-random functions were used to define attributes of the layers. The grading material and other types of attribute distribution can be modeled in a similar way.

Specialized software tools have been developed to model and visualize such hypervolumes. An extension of HyperFun language [29] was introduced in [2] for modeling arbitrary point attributes along with geometry. A polygonizer for the surface mesh generation and a HyperFun plug-in to POVRay are used for visualization.

As these tools are dedicated to surface rendering, we also combined the HyperFun language with vlib [30], a volume graphics API based on CVG. As it was mentioned previously, in CVG, geometry and attributes are deeply connected, and namely the opacity attribute defines in some sense the geometry. To use that API with our model, we have to conform to the CVG definitions. To do so, one has to simply map the attributes of the extended real space $\Re_\theta$ to the default CVG attributes, e.g., an opacity factor equal to 0 for full transparency. In this way, any HyperFun model with attributes can be rendered using vlib to obtain images of objects with varying material distribution inside as in Fig. 9. It is possible to convert this functional model to a 2D cellular complex using surface polygonization of the entire solid or of an individual layer. The next step is to use this surface discretization to generate a 3D cellular complex using advancing front tetrahedrization algorithms [28].

4.2 Adaptive Mesh Generation

We present here examples concerning adaptive mesh generation to illustrate the treatment of attributes other than material distributions. From the theoretical point of view, the presented application is based on the conversion between a functionally defined 2D object with a FRep based attribute to a 2D cellular complex (triangular mesh) described by CRep. The next step is made to a one dimension higher problem, where the object attributes and the resulting cellular complex become time-dependent.

Unstructured grids have found widespread use in computational physics, visualization and data interpolation. In particular , these grids are widely used in finite element modeling in such demanding applications as computational fluid dynamics (CFD), computational structural dynamics (CSD), computational electro-magnetics (CEM) and computational thermo-dynamics (CTD). An accurate numerical solution requires the domain being discretized sufficiently to describe the geometry and physics of the problem. The geometrical compatibility can be achieved by automatic mesh refinement in regions of high curvatures of the boundary surface or contour. The physical compatibility dictates a close correlation between the size and shape of mesh cells and the behavior of the solution that is sought. A varying density of mesh elements can be used to model complex problems with high accuracy. The appropriate element size distribution may be prescribed by the user if he has knowledge of the physical situation a priori. But it is often the case that the detailed information is not available prior to the numerical simulation. In these cases, the element size distribution is provided by a mesh size prediction algorithm in the adaptive analysis procedure. The information about the desired element size and shape is used by mesh generation algorithms.

It may be necessary to describe appropriate element size not only on the boundary but also in some spatial regions inside the domain (e.g., heat-source, oblique shock in supersonic flow, etc.). One of the techniques commonly used for these purposes is based on so-called *sources* [28]. The element size for a location X in the domain is given as a function of the closest distance to source $\rho(X)$. Typically, a small element size is desired close to the source, and a large element size is more preferable far from it. Moreover, the element size should be, in many cases, constant (and small) in the vicinity $\rho<\rho 0$ of the source. Power, exponential or polynomial functions of ρ [28] are usually used to specify the proper element size. Given a set of m sources, the minimum element size computed for each of them is taken whenever an element is to be generated. For moving bodies (solid, liquid, gaseous), the points defining the relevant sources may be synchronized in their movement with the movement of the respective body. This allows for high quality remeshing for non-stationary problems.

Let us consider the application of hypervolumes with a functional model of attributes for the description of mesh elements density. We assume that an attribute $S(X)$ is defined everywhere in the space R^n and an arbitrary value $S_j=S(X_j)$ is interpreted as the desired mesh element size at the point X_j. Geometry of the sources is specified by *FRep*. Then, we can use a value of the function describing the source at a point X as a measure of the closest distance from X to the source, $\rho(X)= \rho(F(X))$. For example, the shape of a point-source may have the following functional definition: $F(x)=a - |X-X0| \geq 0$, where $X0$ is the center of the source, a is its radius, $|X-X0|$ is the distance between the points X and $X0$. Here, we use normalized $F(X)$ so $\rho(X)=F(X)$. An analogous functional description can be created for sources of different shapes. The element size attribute A_i generated by the i^{th} source is defined in the following way:

$$M_{A_i} = (\Re, S_i), \quad where \quad S_i : E^2 \to \Re$$

$$S_i(X) = \begin{cases} h_{\min}, & if \quad F_i(X) \geq 0 \\ \min(h_{\max}, (F_i(X) * (k_i - 1) + h_{\min}) / k_i) & if \quad F_i(X) < 0 \end{cases}$$

This formula provides the geometrical progression law of the element size increase. Here h_{min}, and h_{max} are the minimal and maximal admissible sizes of the elements and k_i is the coefficient of the progression $(k_i \geq 1)$, $Fi(X)$ is the functional description of the i^{th} source. The overall element size distribution (mesh density) attribute A depending on all m sources is calculated as follows

$$M_A = (\Re, S), \quad where \quad S : E^2 \to \Re$$

$$S(X) = \min(S_1(X), \ldots S_m(X)), \qquad X \in \Re^2$$

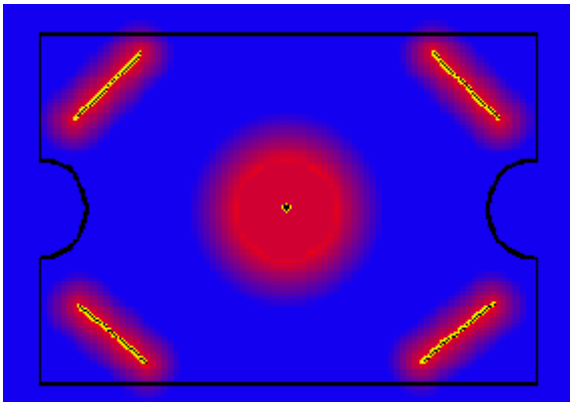

Figure 10: Distribution of the mesh density attribute values for the heat transfer simulation.

Figs. 10, 11 illustrate the example concerning the heat transfer problem. In this example, it is necessary to generate an adaptive mesh in the two-dimensional object shown in Fig. 10. The domain geometry is described by *FRep* as follows:

$F(X) = F_{\square} \wedge_0 (-F_{o1}(X)) \wedge_0 (-F_{o2}(X))$, , where

$F_{\square}(X)$ describes the rectangle, $F_{o1}(X)$, $F_{o2}(X)$ define left and right holes, and the symbol $\wedge_0$ stands for the R-function defining set-theoretic intersection (see 4.1). Taking into account the problem's conditions, we have introduced five mesh density sources (one of the point and four of the segment types) which coincided with the heat sources. The sources' locations are shown in Fig. 10 with color distribution visualizing the corresponding distribution of the element size attribute values. The element size attribute was used for automatic mesh generation based on the advancing front technique. The final mesh is shown in Fig. 11.

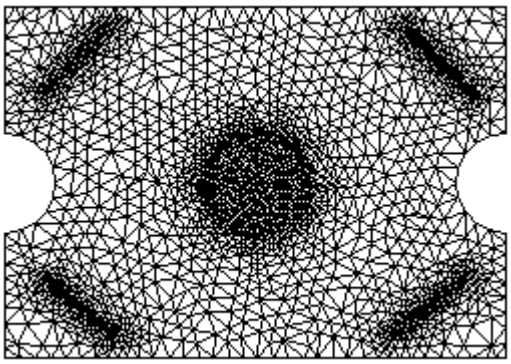

Figure 11: Adaptive mesh for the heat transfer simulation.

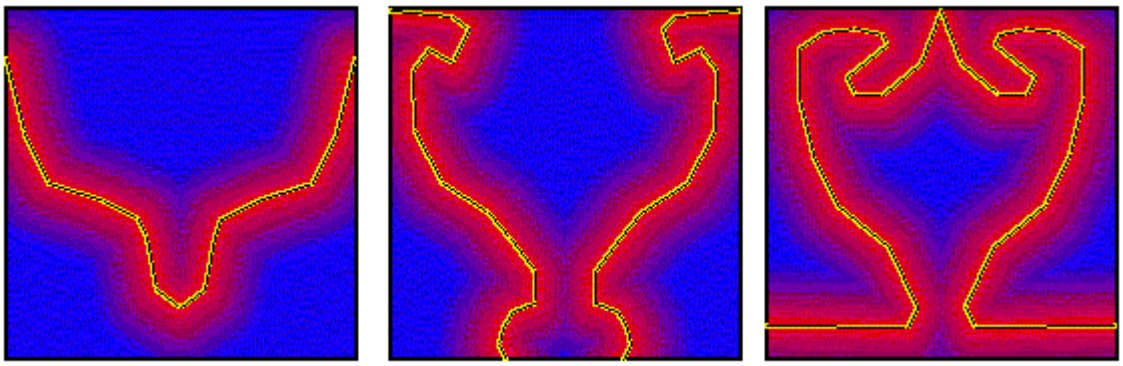

Figure 12: The distribution of the mesh density attribute values for various time-steps in the numerical simulation of the Rayleigh-Taylor instability.

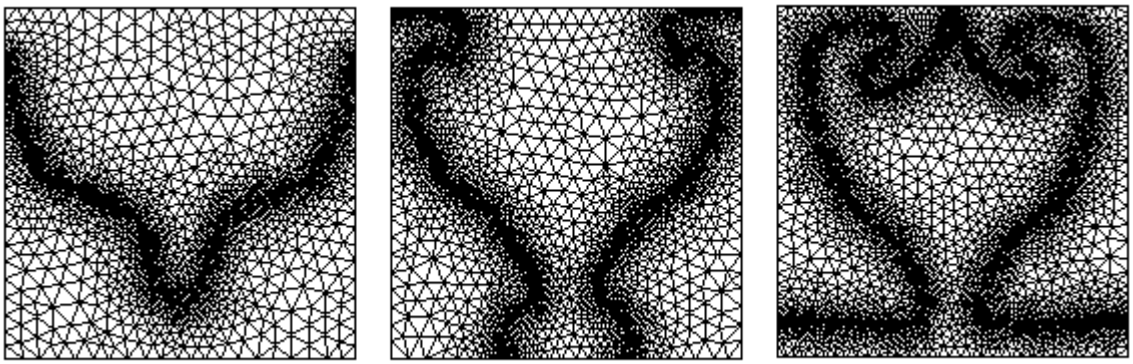

Figure 13: The adaptive meshes for various time-steps in the numerical simulation of the Rayleigh-Taylor instability.

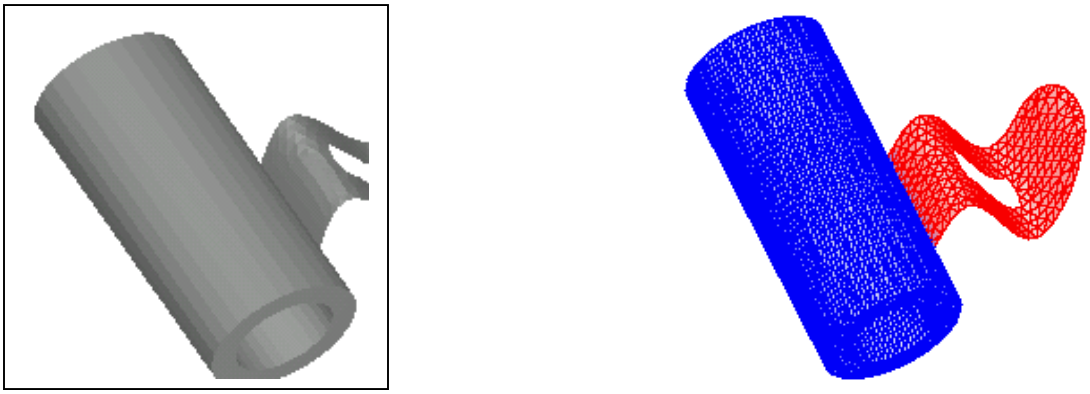

a b

Figure 14: Discretization of a heterogeneous object in E^3: (a) initial Hrep object; (b) discretized Crep object with attributes shown in different colors (brightness in grayscale).

Figs. 12, 13 illustrate the generation of a time-dependent mesh for simulation of the nonlinear stage of the Rayleigh-Taylor instability in the gravitational field. In this example, we have a rectangular domain consisting of two different materials – heavy (upper) and light (lower) gases. The mesh density sources are placed along the interface between the two different gases and is described on the base of the material attribute that in its turn is defined by time-dependent CFRep. The source locations cannot be prescribed beforehand, so they are determined automatically during the numerical simulation. The series of pictures in Figs. 12, 13 show the element size distribution and the corresponding adaptive meshes for various time steps.

4.3 Discretization of 3D heterogeneous object

This case study deals with a problem of discretization of 3D heterogeneous objects that is quite important in the context of many applications, especially associated with computational structural dynamics. The object to be discretized (see Fig. 14a) was introduced in 3.1.3 and is the simplified component of the mixing tank impeller which is used as the agitator of the flow components in a chemical reactor. Its geometry was represented as HRep in the form of the implicit complex (see Fig. 4 and the associated formulae). In terms of the cellular-functional framework the discretization means converting HRep into CRep. Such a procedure can include the following steps:

- One-dimensional cell $e^1{}_1$ and its preimage cell $(e^1{}_1)'$ are subdivided;
- Discretization of 2D point set $(T_2{}^2)'$ conforming to the subdivision of edge $(e^1{}_1)'$ thus yeilding a triangle mesh on the plane (u,v) ;
- This 2D mesh is mapped into E^3 through homeomorphism h yielding the decomposed domain D_2;
- Discretization of domain D_2 conforming to the subdivision of edge $e^1{}_1'$;
- Finally, the complexes describing discretization of the both domains are combined into the resulting CRep of the object. Fig. 14b shows the object with the material attribute described by a CFRep in Section 3.2.2. Here, blue color corresponds to material of index μ_1 and red color is used to denote material of index μ_2 (materials are shown by different brightness in grayscale).

The test examples were prepared using the software tools intended for the data preprocessing in computational physics [31]. These tools provide input/output CRep of the initial boundary and the resulting decomposition, interactive specification of the mesh density sources described by FRep, automatic mesh generation on the base of the advancing front method, mesh optimization including Laplacian smoothing and edge swapping, generation of the dual Dirichlet tessellation. The tools are being integrated with HyperFun tools into a single environment.

5. CONCLUSION

Let us summarize the main contributions of this work. In this paper, we

- used multidimensional point sets with multiple attributes (hypervolumes) as a base for modeling of heterogeneous objects;
- introduced rigorous topological framework as a solid mathematical base for independent but unifying representation of geometry and attributes;
- proposed both a functional and a cellular representation to model objects, which are heterogeneous in their dimensionality and internal structure defined by attributes;
- described the functional and cellular models of object geometry and attributes on the base of the rigorous survey and classification of relevant topological notions;
- introduced and discussed a hybrid cellular-functional model by using the notion of an implicit complex;
- provided the case studies of modeling heterogeneous objects using the functional and cellular representations supported by original experimental software.

As cellular-functional modeling is a new research direction, a lot of work should be done, and we will continue our research on the models as well as development of the corresponding software tools and applications.

6. ACKNOWLEDGMENTS

The authors sincerely thank professors P. Comninos and J.J. Zhang (NCCA, Bournemouth University, UK), V. Gasilov (Institute for Mathematical Modeling, Russian Academy of Science) and C. Schlick (LaBRI, Bordeaux University, France) for their support of this work. The comments by anonymous referees helped us significantly improve the paper. Our special thanks go to professor E. Sandrakova (Moscow Engineering Physics Institute, Russia) for useful discussions of topological problems, professor M. McDonald (Hosei University, Japan) for the linguistic expertise of the title, and Jody Vilbrandt for making the text more reader friendly.

7. APPENDIX

Topological Framework

Let us introduce some necessary topological notions summarized on the basis of a number of sources [25, 32-36]. More complete description of this framework can be found in [37].

A topological space X is called a *cellular space* if it can be represented as the union of nonintersecting sets e_i^q , called *cells* (where q is the dimension of the cell and i is its index number) $X = \bigcup_{q=0}^{n} (\bigcup_{i=1}^{m_q} e_i^q)$, and the following conditions are satisfied:

1) The closure $\overline{e_i^q}$ of each cell e_i^q is the image of the closed q-dimensional ball $\overline{B^q}$ under some continuous and surjective map $\chi_{iq} : \overline{B}^q \to \overline{e}_i^q$ called the *characteristic map* of the given cell;
2) The restriction of χ_{iq} on the open ball B^q is a *homeomorphism* between B^q and e_i^q ;
3) The *boundary* of each cell, that is the set $\partial e_i^q = \overline{e}_i^q - e_i^q$ is the image of the boundary ∂B^q of the ball B^q , so that $\partial e_i^q = \chi_{iq}(\partial B^q)$. It is contained in the union of a finite number of cells of lesser dimensions;
4) A subset Y in X is closed if and only if each inverse image $\chi_{iq}^{-1}(Y)$ is closed in the ball $\overline{B^q}$ for any cell e_i^q .

Such a cellular structured space is called *CW-space* [35] ("CW" stands for "Closure-finite with the Weak topology"). The *p-skeleto*n of X consists of cells, whose dimensions do not exceed p. Each skeleton X^{p-1} is a subspace of X^p. For any cellular space X we can get a sequence of skeletons Xp, such that

$X^o \subseteq X^1 \subseteq \ldots \subseteq X^p \ \ldots \subseteq X$; $X = \bigcup_{p=0}^{n} X^p$

This sequence is called *filtration*.

A collection K of cells forming a CW-space X and satisfying the conditions listed above is called a *CW-complex*. So, $K = \{e_i^q\},\ q = \overline{0,n};\ i = \overline{1,m_q}$.

Then, X is called a *carrier* or an *underlying space* of K. It is denoted accordingly as K=Ξ(X) and X=|K|. The *dimension* of K is the maximal dimension of the cells of X.

Depending on restrictions on cell geometry and types of characteristic maps, complexes of other types can similarly be defined. In particular, one can deal with *simplicial complexes*, *polyhedral complexes* (with cells composed of convex polytopes) and *cell (curvilinear) complexes* (with cells homeomorphic to polytopes). In some applications, very special cell geometry and restricted types of maps can allow for designing efficient algorithms dealing with complexes. Building the framework based on CW-complexes, one can imply that all the conclusions can easily be applied to complexes of other types.

A subset L of cells of the CW-complex K ($L \subseteq K$) is a CW-complex called a *subcomplex* of K, if and only if for each cell $e_i^q \in K$ either $e_i^q \cap L = \varnothing$ or $\overline{e_i^q} \in L$. The corresponding cellular space |L| is a closed subspace of |K|, $|L| \subseteq |K|$. Union or intersection of any subcomplexes L , $M \subseteq K$ is a subcomplex of K. We state that two cellular complexes A and B are *properly joined* if either $A \cap B = \varnothing$ or $A \cap B = C$, where C is a subcomplex of both A and B. Union of properly joined cellular complexes is also a cellular complex. The similar assertion is true regarding the corresponding cellular spaces.

A cellular space can be composed via attaching cells [18, 34]. This procedure has a constructive nature and can be very useful in composing models within the cellular-functional framework.

8. REFERENCES

[1] Pasko, A., Adzhiev, V., Schmitt, B., Schlick, C. Constructive hypervolume modelling, Graphical Models, special issue on Volume Modeling, 63(6), 2001, 413-442.

[2] Pasko, A., Adzhiev, V., Schmitt, B. Constructive hypervolume modelling, Technical Report TR-NCCA-2001-01, National Centre for Computer Animation, Bournemouth University, UK, ISBN 1-85899-123-4, 2001, 34 p.
URL: http://wwwcis.k.hosei.ac.jp/~F-rep/BTR001.pdf

[3] Kumar,V., Dutta, D. An approach to modeling multi-material objects, Fourth Symposium on Solid Modeling and Applications, ACM SIGGRAPH, 1997, 336-345.

[4] Kumar, V., Burns, D., Dutta, D., Hoffmann, C. A framework for object modeling, Computer-Aided Design, 31(9), 1999, 541-556.

[5] Shin, K., Dutta, D. Constructive representation of heterogeneous objects, Journal of Computing and Information Science in Engineering, 1(3), 2001, 205-217.

[6] Chen, M., Tucker, J. Constructive volume geometry, Computer Graphics Forum, 19(4), 2000, 281-293.

[7] Jackson, T. R., Liu, H., Patrikalakis, N. M., Sachs, E. M., and Cima, M. J. Modeling and designing functionally graded material components for fabrication with local composition Control, Materials and Design, 20(2/3), 1999, 63-75.

[8] Martin, W., Cohen, E. Representation and extraction of volumetric attributes using trivariate splines: a mathematical framework, Sixth ACM Symposium on Solid Modeling and Applications, D. Anderson, K. Lee (Eds.), ACM Press, 2001, 234-240.

[9] Park, S. M., Crawford, R., Beaman, J. Volumetric multi-texturing for functionally gradient material representation, Sixth ACM Symposium on Solid Modeling and Applications, D. Anderson, K. Lee (Eds.), ACM Press, 2001, 216-224.

[10] Pasko, A., Adzhiev, V., Sourin, A., Savchenko, V. Function representation in geometric modelling: concepts, implementation and applications, The Visual Computer, 11(8), 1995, 429-446.

[11] Paoluzzi, A., Bernardini F., Cattani, C., Ferrucci, V. Dimension-independent modeling with simplicial complexes, ACM Transactions on Graphics, 12(1), 1993, 56-102.

[12] Arbab, F. Set models and boolean operations on solids and assemblies. IEEE Computer Graphics and Applications, 10(6), 1990, 76-86

[13] Rossignac, J., O'Connor, M. SGC: a Dimension independent model for pointsets with internal structures and incomplete boundaries, In Geometric modeling for product engineering, ed. by M. Wozny, J. Turner, K. Preiss, 1990.

[14] Armstrong, C., Bowyer, A., Cameron, S. et al. Djinn. A Geometric Interface for Solid Modeling, Information Geometers, Winchester, UK, 2000.

[15] Grimm, C.M., Hughes, J.F. Modeling surfaces of arbitrary topology using manifolds, Computer Graphics (SIGGRAPH '95 Proceedings), 1995, 359-368.

[16] Hart, J. Using the CW-complex to represent the topological structure of implicit surfaces and solids. Proc. Implicit Surfaces '99, Eurographics/SIGGRAPH, 1999, 107-112.

[17] Kunii, T. Valid computational shape modeling: design and implementation, International Journal of Shape Modeling, 5(2), 1999, 123-133.

[18] Ohmori, K., Kunii, T. Shape modeling using homotopy, International Conference on Shape Modeling and Applications, IEEE Computer Society, 2001, 126-133.

[19] Nielson, G. Volume modeling. In Volume Graphics, ed. by Chen, M., Kaufman, A., Yagel, R., Springer-Verlag, 2000, 29-48.

[20] Adzhiev, V., Kazakov, M., Pasko, A. Savchenko, V. Hybrid system architecture for volume modeling, Computers and Graphics, Pergamon Press, 24(1), 2000, 67-78.

[21] Rvachev, V. Theory of R-functions and some applications, Naukova Dumka, Kiev, 1982 (in Russian).

[22] Rvachev, V.L., Sheiko, T.I., Shapiro, V., Tsukanov, I. Transfinite interpolation over implicitly defined sets, Computer-Aided Geometric Design, 18, 2001, 195-220.

[23] Shapiro, V., Tsukanov, I. Implicit functions with guaranteed differential properties, Proceedings of the Fifth ACM Symposium on Solid Modeling and Applications, ACM, 1999, 258-269.

[24] Shapiro, V., Tsukanov, I. Meshfree simulation of deforming domains, Computer Aided Design, 31(7), 1999, 459-471.

[25] Fomenko, A.T., Kunii, T.L. Topological modeling for visualization, Springer-Verlag, Tokyo and Heidelbrg, 1997.

[26] Kartasheva, E. Reduction of h-genus polyhedrons topology, International Journal of Shape Modeling, 5(2), 1999, 179-194.

[27] Pasko, A., Pilyugin, V., Pokrovskiy, V. Geometric modeling in the analysis of trivariate functions, Computers and Graphics, 12(3/4), 1988, 457-465.

[28] Löhner, R., Automatic unstructured grid generators, Finite Elements in Analysis and Design, vol. 25, 1997, 111-134.

[29] Adzhiev, V., Cartwright, R., Fausett, E., Ossipov, A., Pasko, A., Savchenko, V. HyperFun project: a framework for collaborative multidimensional F-Rep modeling. Proc. Implicit Surfaces '99, Eurographics/ACM SIGGRAPH Workshop, ed. by Hughes, J., Schlick, K., 1999, 59-69.

[30] Winter, A., Chen, M. vlib: A volume graphics API, Proceedings of the 2-nd International Workshop on Volume Graphics, New York, 2001, 81-90.

[31] Kartasheva, E. Instrumental data preparation and analysis software for solution of 3D mathematical physics problems, Mathematical Modeling Journal, Moscow, 1997, 9(7), 113-127 (in Russian).

[32] Alexandrov, P.S. Combinatorial Topology, OGIZ, Gostehizdat, Moscow, 1947 (in Russian).

[33] Whitehead, J.H.C. Combinatorial homotopy, I. Bull. Amer. Math. Soc., 55, 1949, 213-245.

[34] Massey, W.S. Algebraic topology: An introduction. Harcourt, Brace&World, Inc., New York-Chicago-San Francisco-Atlanta, 1967.

[35] Fritsch, F., Piccinini, R.A. Cellular structures in topology. Cambridge University Press, Cambridge, 1990.

[36] Handbook of Discrete and Computational Geometry, ed. by Goodman J., O'Rourke J., CRC Press, 1997.

[37] Adzhiev, V., Kartasheva, E., Kunii, T., Pasko, A., Schmitt, B. Cellular-functional modeling of heterogeneous objects, Proc. ACM Solid Modeling and Applications 2002 Symposium, Saarbryucken, Germany, Ed. Kunwoo Lee, N. Patrikalakis, ACM Press, 2002, 192-203.